Eur. Phys. J. B **62**, 87–94 (2008)
DOI: 10.1140/epjb/e2008-00126-9

THE EUROPEAN PHYSICAL JOURNAL B

Locals vs. global synchronization in networks of non-identical Kuramoto oscillators

M. Brede[a]

Centre for Complex Systems Science, CSIRO Marine and Athmospheric Research, GPO Box 284, Crace Canberra, ACT 2601, Australia

Received 3 December 2007 / Received in final form 11 February 2008
Published online 21 March 2008 –

Abstract. In this paper networks that optimize a combined measure of local and global synchronizability are evolved. It is shown that for low coupling improvements in the local synchronizability dominate network evolution. This leads to an expressed grouping of elements with similar native frequency into cliques, allowing for an early onset of synchronization, but rendering full synchronization hard to achieve. In contrast, for large coupling the network evolution is governed by improvements towards full synchronization, preventing any expressed community structure. Such networks exhibit strong coupling between dissimilar oscillators. Albeit a rapid transition to full synchronization is achieved, the onset of synchronization is delayed in comparison to the first type of networks. The paper illustrates that an early onset of synchronization (which relates to clustering) and global synchronization are conflicting demands on network topology.

PACS. 89.75.-k Complex systems – 05.45.Xt Synchronization; coupled oscillators – 89.75.Fb Structures and organization of complex systems

1 Introduction

Synchronization problems occur in a multitude of contexts, having applications in fields ranging from biology, ecology, semiconductor lasers to social collective behaviors [1–4]. A convenient framework to study synchronization goes back to the seminal work of Kuramoto [5], who studied the synchronization of limit cycle oscillators via

$$\dot{\phi}_i = \omega_i + \sigma \sum_j a_{ij} \sin(\phi_j - \phi_i). \tag{1}$$

In equation (1) the $\phi_i, i = 1...N$ describe the phases of the N oscillators, the ω_i's the oscillators' native frequencies while σ gives the coupling strength and the a_{ij} the structure of the coupling architecture. The coherence of the N oscillators can be measured by the order parameter

$$r(t)\exp(i\phi(t)) = 1/N \sum_j \exp(i\phi_j(t)), \tag{2}$$

where $\phi(t)$ is the average phase and $0 \leq r \leq 1$ is a measure for the phase coherence of the oscillators. Note, that $r(t)$ measures the coherence between *all* oscillators.

One interesting aspect that has recently found much interest is synchronization in systems with heterogenous coupling architectures a_{ij} described by complex networks. Given a network, the coupling matrix a_{ij} can be identified with its adjacency matrix $a_{ij} = 1$ if node i is linked to node j and $a_{ij} = 0$ otherwise. In this paper we will restrict ourselves to symmetrical matrices, i.e. undirected networks.

Relating the structure and properties of the network to synchronization properties is a field of very active research [6–25]. One pillar of this research are studies improving the understanding of the stability of the fully synchronized state via the Master Stability Function approach pioneered by Pecora et al. [6]. From such analysis it is found that topologies with very small average pathlength and a very democratic structure characterized by homogeneity in the degree distribution have the highest stability of the fully synchronized state [17,19]. Recently, these results have been extended to different types of weighted networks [14,18]. While much insight has been gained in this way, the method is restricted to studying systems of identical oscillators and is not able to describe the interesting dynamics on the way towards the fully synchronized state.

Heterogeneity in the distribution of the native frequencies, however, is the more common case in applications of the synchronization problem in many, particularly biological or ecological, contexts. Nontrivial couplings of the oscillators have been extensively studied [6–25], but correlations in the arrangement of oscillators on the nodes have rarely found interest so far. However, in [25] it has been

[a] e-mail: Markus.Brede@Csiro.au

shown that the synchronization properties of a network and native frequency arrangement are indeed critically influenced by correlations in the oscillators placement.

In this recent work we have developed a numerical method for constructing networks of non-identical Kuramoto oscillators with optimal synchronization properties. While the framework does not have the generality of the eigenratio analysis, insights about the connection between heterogeneity in the distribution of native frequencies and the network structure can be gained. The analysis in [25], however, also concentrates on the fully synchronized state. In this paper we build upon this work, extending it towards addressing issues of local synchronization and the onset of synchronization.

It has recently been pointed out that synchronization properties of networks depend critically on the entire range of coupling strengths [22–24]. While some networks exhibit an early onset of synchronization, the fully synchronized state can be unstable. On the other hand networks with very stable fully synchronized states may exhibit a delayed onset of synchronization in comparison to the latter. This phenomenon is further detailed in references [23,24], which introduce the average pairwise coherence of linked oscillators

$$r_{\text{link}} = 1/L \sum_{(k,l)} \left| \lim_{\Delta T \to \infty} 1/\Delta T \int_{T_{\text{rel}}}^{T_{\text{rel}}+\Delta T} e^{i(\phi_l(t)-\phi_k(t))} dt \right|, \tag{3}$$

as an additional synchronization measure. In (3) the sum extends over all edges (k, l) of the network and L is the number of links. T_{rel} denotes the relaxation time and ΔT the time over which the coherence between adjacent oscillators is measured. It is shown that r_{link} can pick up information about the way to synchronization in a regime where $r \approx 0$, i.e. where no systemwide synchronization has occured yet.

While the above order parameter r is a measure for the *global* synchronization, r_{link} can be interpreted as a measure for *local* synchronization. Whereas r measures the coherence between all pairs of oscillators, r_{link} only measures the degree of synchronization between pairs of adjacent oscillators. While both provide the same information in fully coupled systems, they may differ substantially particularly when the coupling occurs via a sparse network. Clearly, $r_{\text{link}} = 1$ when $r = 1$. However, a network may have $r_{\text{link}} \approx 1$ while $r \ll 1$. Such a situation is found in networks with strong community structures, where modules can be synchronized in themselves but not with each other. Indeed, building on this property, it has been demonstrated that r_{link} can be used to detect community structures in networks [26,27]

Recently, two methods for evolving networks of non-identical oscillators towards enhanced synchronizability have been proposed. In reference [20] the authors consider a procedure that rewires networks with a bias towards connecting oscillators with similar average frequencies. One major outcome of this work is that for intermediate coupling strength non-trivial network structures characterized by a high level of cliquishness and large average distances emerge. This contrasts with the networks exhibiting an early transition to the fully synchronized state generated with a different rewiring algorithm in [25] or such displaying optimal stability of the synchronized state [17,19]. These networks are found to be very small, homogeneous in degree and not cliquish. A further important finding of [25] is that such networks are characterized by anticorrelated native frequencies on adjacent nodes.

In this paper we use the methods developed in [25] to evolve networks that realize different trade-offs between local and global synchronizability. The outcome of the evolution procedure is found to be strongly influenced by the coupling strength. We show that strongly cliquish large networks with distinct community structures of oscillators with similar native frequencies emerge when the coupling strength is low, while the small networks with anticorrelated adjacent oscillators without community structures arise for large coupling strengths. In the first case, local synchronizability is favored over global synchronizability during the network evolution. In the second case, the network evolution is guided by improvements in the global synchronizability.

2 Evolving networks with global and local synchronizability

2.1 Evolution procedure

In the following we study the trade-off between local and global synchronizability of networks. For this purpose we define a network's synconizability for a given coupling strength σ^* by

$$R(\sigma^*) = \lambda r(\sigma^*) + (1-\lambda) r_{\text{link}}(\sigma^*) \tag{4}$$

as a convex combination of local and global synchronizability. In this definition (4) the quantities R, r and r_{link} are first understood as the respective values for homogeneous initial conditions $\phi_i(t = 0) = 0, i = 1, ..., N$. However, it turns out that configurations with an enhanced value of R for homogeneous initial conditions also have an enhanced value of R averaged over heterogeneous initial conditions. The reason for this appears to be that the main counterforce against synchronization stems from the heterogeneity in the native frequency distribution of the oscillators.

We proceed by using the method described in [25] to generate network topologies that maximize R for different coupling strengths σ^*. Essentially, starting from an Erdös-Rényi type (ER) random network [28] and native frequencies randomly drawn from a uniform distribution over $[-1, 1]$ the evolution procedure consists of the following steps.

1. Integrate equations (1) with initial conditions $\phi_i(t = 0) = 0, i = 1, ..., N$ over the time interval $[0, T_{\text{rel}} + \Delta T]$. The time interval $[0, T_{\text{rel}}]$ is for relaxation and average local and global synchronizability

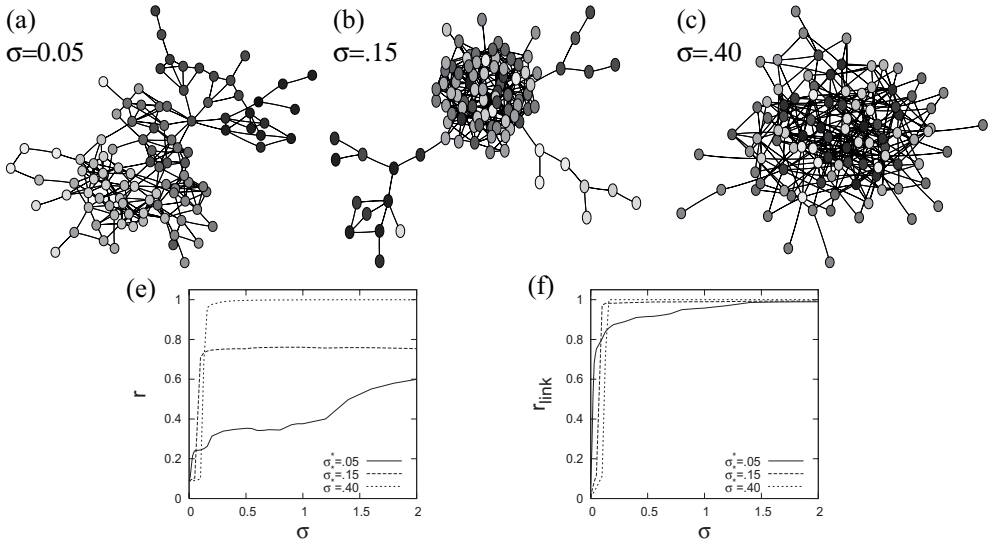

Fig. 1. Example networks with optimal synchronizability R constructed for (a) low coupling strength (b) intermediate coupling strength and (c) large coupling strength for $\lambda = 1/2$ (equal share of local and global synchronizability in R). Parameters are $N = 100, \langle k \rangle = 5$. The color of the nodes corresponds to the native frequency of the node, white nodes have $\omega = -1$ and black nodes $\omega = 1$ while different shades of gray interpolate between both situations. The lower panels (e) and (f) show the dependence of the global and local synchronizability on the coupling strength σ for the networks (a–c). Data points represent averages over 100 random initial conditions of the phases.

r_{link} and $\overline{r}$ are calculated over $[T_{\text{rel}}, T_{\text{rel}} + \Delta T]$ to determine R. This defines the 'fitness' of the current network configuration. For all the following simulations $T_{\text{rel}} = 200$ and $\Delta T = 200$ are used.

2. A rewired network, where l randomly picked links are swapped to l link vacancies is suggested, provided it is connected. Then its fitness R is determined via step 1. The network configuration is accepted if it gives rise to an improvement in the synchronizability measure R and rejected otherwise.
3. Step 2. is repeated till no improvement in R was found over the last $L = 1/2 \sum_{i,j} a_{ij}$ iterations. Starting from $l \approx 10$ the number of rewired links l is gradually reduced to narrow down the search space. Typically, about 10 000 iterations of step 2. are performed.

Figure 1 gives three example networks generated for small, intermediate and large coupling strength and $\lambda = 1/2$. Clearly, the network generated for low coupling (Fig. 1a) exhibits a strong community structure marked by a modular grouping of nodes with similar native frequencies. The interfaces or bridges between the groups are typically small which leads to large average distances between nodes. For the example network of Figure 1a one observes an almost linear structure, where the native frequencies of oscillators gradually change from $\omega = -1$ to $\omega = 1$ from left to right. In this sense oscillators with large frequency magnitudes are at the periphery of the network. In contrast, the network evolved for large coupling strength shown in Figure 1c appears tightly connected, small and without any apparent community structure. Closer inspection shows that native frequencies on adjacent nodes are not positively correlated as for Figure 1a, but anticorrelated. One also observes that now large and very low frequency oscillators (black and white nodes) are in the centre of the network, while oscillators with close the zero frequency magnitudes (intermediate shade of gray) are at the periphery. The network shown in Figure 1b interpolates between the limiting cases of Figures 1a and 1c. A tightly connected core distinguished by on average slightly anti-correlated frequency pairings has been formed. However, at the periphery tree-like structures that loosely couple nodes of positively correlated native frequencies to the core are retained.

In the lower panels (e) and (f) the dependence of the global and local synchronizability on the coupling strength for the example networks are displayed. The network evolved for low coupling (Fig. 1a) exhibits an early onset of a low degree of global synchronization also marked by a very steep increase of the local synchronization measure. Full global synchronization, however, is not achieved for the range of coupling strengths in the figure. Conversely, the network evolved for large coupling (Fig. 1c) shows a later onset of synchronization, but also a rapid transition to the fully synchronized state. The network of Figure 1b is also an intermediate here: it has a slightly earlier onset of synchronization when compared to 1c, but does not achieve full synchronization for moderate coupling strength. Closer inspection, e.g. via an analysis of the coherence matrix

$$d_{ij} = a_{ij} \left| \lim_{\Delta T \to \infty} 1/\Delta T \int_{T_{\text{rel}}}^{T_{\text{rel}}+\Delta T} e^{i(\phi_i(t) - \phi_j(t))} dt \right| \quad (5)$$

introduced in [23,24], shows that the network ends up in a state where the core nodes and the groupings of nodes at the periphery are synchronized intrinsically and full

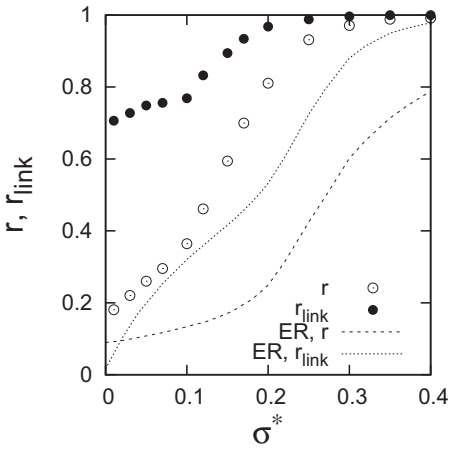

Fig. 2. Dependence of r and $r_{\rm link}$ on the coupling strength σ^* for which the networks were evolved. The curves represent averages over 100 evolved networks (each evolved from a different ER initial network with a different random native frequency selection) and are calculated for random initial conditions. For comparison the $r(\sigma)$ and $r_{\rm link}(\sigma)$ dependencies for the initial ensemble of ER networks are given (dotted and dashed lines).

global synchronization can only be reached for very large coupling.

It is also worthwhile to note the stepwise increases of r and $r_{\rm link}$ for the network (a). This clearly results from the community structure. Steps in the dependence of r and $r_{\rm link}$ on σ represent critical points in the coupling where separate communities become synchronized with each other. As the coupling between the communities is low and typically only happens via only a few connections, distinct communities of oscillators are hard to synchronize. Essentially, this is also the reason why full synchronization is hard to achieve on these networks.

The above findings already illustrate an important point: an early onset of synchronization and a rapid transition to full synchronization are conflicting demands on the network topology. The first is connected to a high degree of local synchronization for low coupling and the existence of small communities of interlinked similar oscillators within the network. The latter requires good mixing and many linkages between dissimilar oscillators.

2.2 Network structures

To explore and strengthen the main point of the previous subsection we repeat the evolution procedure for systematically varied coupling strengths σ^* and consider averages over different realizations of the initial networks and native frequencies.

In Figure 2 the dependence of the local and global synchronizabilities of the optimized networks on σ^* are shown. The data demonstrate that in comparison to the ER seed networks the evolution procedure enhances both local and global synchronizabilities over the entire range of coupling strengths σ^*. However, whereas a large degree of global synchronization can only be achieved for large coupling, a large degree of local synchronization is also achievable for very low σ^*. Initially, both r and $r_{\rm link}$ increase slowly with σ^*. The value $\sigma^* \approx 0.12$ marks a transition, from which onwards strong improvements in the global synchronizability become possible. Below, we shall discuss the changes in network structure that cause the according differences in the system's synchronization behaviour.

For this several quantities are measured to characterize the networks and the arrangement of native frequencies on them. Among these, the clustering coefficient c [29], the average shortest pathlength l and the variance of the degree sequence σ_k^2 are calculated. To better describe the transition of typical networks from multi-community structures (cf. Fig. 1a) to networks without community structure (cf. Fig. 1c) we also compute the number of nodes $n_{\rm tree}$ that belong to tree structures. This is done by recursively removing nodes of degree one.

As in [25] the arrangement of native frequencies on the network can be characterized by the number of adjacent pairs of oscillators with native frequencies of opposite signs, p_- and a correlations coefficient

$$c_\omega = \frac{\sum_{i,j} a_{ij}(\omega_i - \overline{\omega}\rangle)(\omega_j - \overline{\omega})}{\sum_{i,j} a_{ij}(\omega_i - \overline{\omega})2}, \qquad (6)$$

where $\overline{\omega} = 1/N \sum_i \omega_i$ is the average native frequency for a given realization. For the ensemble of random initial Erdös-Rényi networks with $N = 100$ nodes and average degree $\langle k\rangle = 5$ without correlations in the arrangement of the ω_i's one has $\langle c\rangle = 0.05 \pm 0.02$, $\langle l\rangle = 3.0 \pm 0.1$, $\langle\sigma_k^2\rangle = 4.6 \pm 0.5$, $\langle n_{\rm tree}\rangle = 3.4 \pm 0.9$, $\langle p_-\rangle = 0$ and $\langle c_w\rangle = 0$. Note that in the following $\langle\cdot\rangle$ always denotes averages over the ensemble of initial networks and the ensemble of native frequencies.

In Figures 3a–3f simulation data for the dependencies of these network and frequency arrangement characteristics on the coupling strength σ^* for which they were optimized are given. By the data in panels (a)–(f) the gradual transition between locally clustered networks with communities of similar native frequency oscillators to the unclustered frequency anticorrelated pairing with growing coupling strength σ^* is illustrated. For low coupling strength σ^* the clustering coefficient is vary large and oscillators are almost always linked to other oscillators of similar native frequency. Good local synchronizability within the communities can be realized when the disturbing influence from one community on the other is minimized. This is realized when average distances in the network are large, i.e. distinct communities are widely separated and only adjacent to other communities synchronizing to a similar average frequency.

When σ^* is increased the typical size of communities grows, while the average cliquishness still remains relatively large. Some communities incorporate more links, whereas others evolve into tree-like structures, but are composed of oscillators with very similar frequencies. The increasing prominence of tree-like structures can be seen from Figure 3f. From $\sigma^* \approx 0.12$ onwards typically only one unique densely interconnected core-community is found.

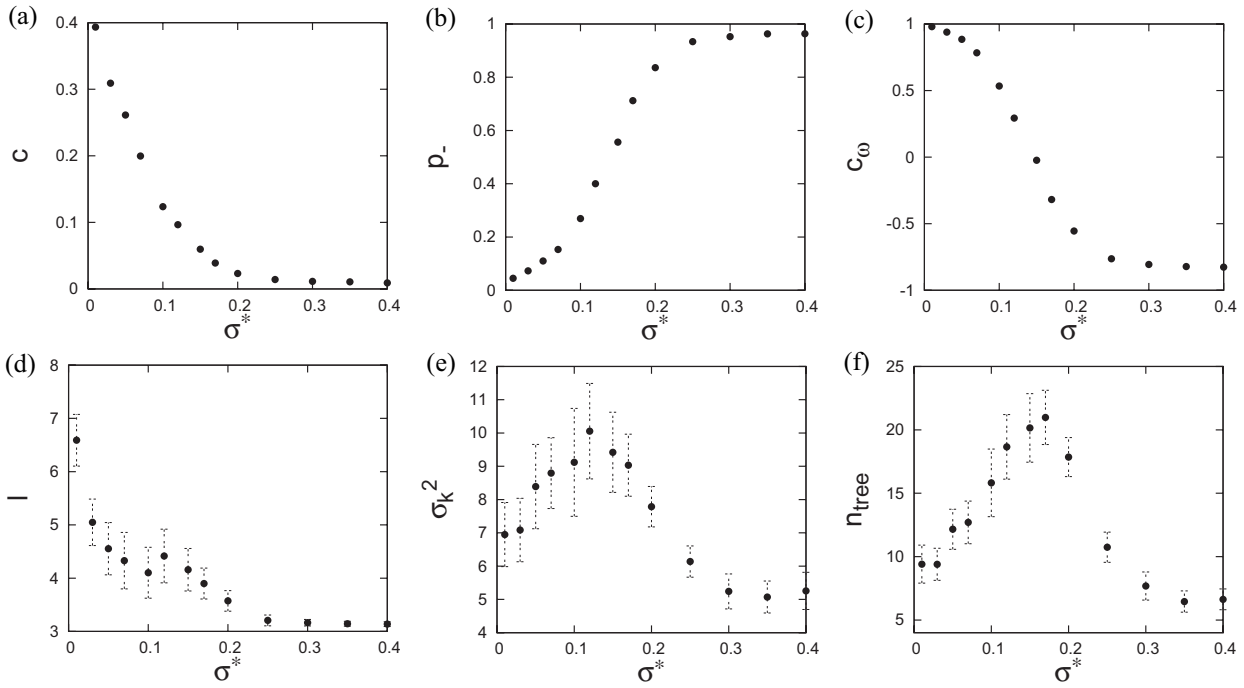

Fig. 3. Dependence of the average (a) clustering coefficient, (b) fraction of adjacent native frequencies of opposite sign, (c) correlation coefficient between adjacent native frequencies, (d) pathlength, (e) variance of the degree sequence, and (d) nodes in tree components on the coupling strength σ^* for which the networks were optimized. All data points represent averages over 100 optimized networks of size $N = 100$ and with $\langle k \rangle = 5$.

This core, which is responsible for a large degree of global synchronization for large coupling, connects to a tree-like periphery, which is further thinned out of links when σ^* is progressively increased. The small periphery still gives an increased measure of local synchronizability for low coupling and the already relatively large core allows for a large degree of global synchronization for large coupling. Increasing σ^* further to roughly $\sigma^* \approx 0.17$ the maximum size of tree-like parts of the networks is reached. At this stage full synchronization is very hard to achieve, since the small tree-like communities are only loosely linked to the core, but strongly supported by similar native frequency oscillators in the trees.

At around $\sigma^* = 0.2$ the periphery quickly starts to disappear and most of the network condenses into only one core. For still larger σ^* the few mainly degree one nodes still in tree-like parts can now contribute towards full synchronization, because they lack the previous support of similar native frequency oscillators at the end of the chains. This is seen from a first steep increase of r at the transition, which is then followed by a gradual approach towards $r = 1$ for growing coupling.

Further proof for the transition from cliquish networks towards core-periphery networks with tree-like peripheries to networks without community structure is found in the degree distributions of the networks (see Fig. 4). For low coupling the distribution proves to be relatively heterogeneous, there are hub nodes in the centres of communities and low degree nodes connecting them. For intermediate coupling nodes of low degree, chiefly degree one or two rise in prominence. They are typically either leaves of trees or

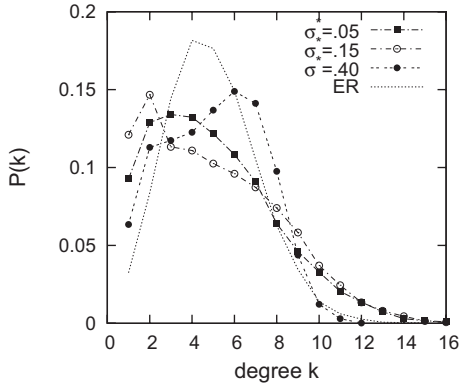

Fig. 4. Degree distribution for networks constructed for several values of σ^*. For comparison the degree distribution of the initial Erdös-Rényi type networks is also shown (ER). The distributions are constructed from sets of 100 optimized networks for each σ^*.

involved in long chains in the trees. For larger values of σ^* trees and with them low degree nodes gradually disappear and the networks become very homogeneous.

A further interesting observation is that degree and native frequency magnitude correlate in different ways on networks optimized for low and large coupling. To examine this we plot the dependence of the average native frequency magnitude $|\omega(k)|$ on the degree k, cf. Figure 5. One notes that for the networks evolved for low coupling low degree nodes are typically associated with large magnitude native frequencies. Thus nodes with large native frequency magnitudes tend to be situated at the periphery of

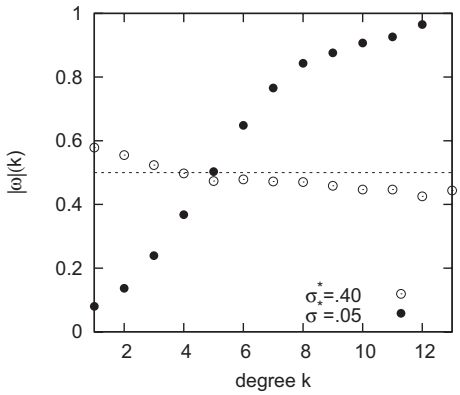

Fig. 5. Dependence of the average absolute value of the native frequency $|\omega|(k)$ on the degree for networks evolved for small and large coupling. For large coupling large native frequencies are associated with large degrees but for small coupling a small correlation to the opposite is observed. The line $|\omega|(k) = 0.5$ gives the expectation for an uncorrelated ensemble. Data averaged over 100 evolved networks in each case.

the network. This contrasts with the opposite correlation for networks evolved for large coupling. In these larger degree nodes typically also have larger native frequencies, i.e. large native frequencies tend to be in the centre of the network. An explanation for this is that such an arrangement actually favors a larger degree of anticorrelation between adjacent native frequencies of oscillators.

2.3 Spectral analysis

Albeit it neglects correlations between network topology and oscillator identity a spectral analysis of the evolved networks also proves insightful. From the symmetric coupling matrix a_{ij} the network's Laplacian matrix G can be constructed via

$$g_{ij} = \begin{cases} a_{ij} & \text{if } i \neq j \\ -\sum_j a_{ij} & \text{otherwise} \end{cases}. \qquad (7)$$

Since we assume symmetric real coupling all eigenvalues of G are real and non-negative. They can be ordered as $0 = e_0 \leq e_1 \leq ... \leq e_N = e_{\max}$. For connected networks one has $e_{\min} = e_1 > 0$. Generally, the number of zero eigenvalues of G gives the number of connected components of the corresponding networks. Eigenvalues of G close to zero indicate a network structure close to disconnected components. Hence, loosely connected community structures manifest themselves by gaps between small eigenvalues [26].

In Figure 6a the spectrum of networks evolved for different σ^* is shown. One notes, that networks evolved for small σ^* have many eigenvalues close to zero. The number of close to zero eigenvalues then decays as σ^* is increased till the narrow compact spectra characterizing globally synchronizable networks are reached. Community structures referred to above are groupings of connected oscillators with similar native frequencies. Even though the identity of oscillators is not reflected in the Laplacian matrix,

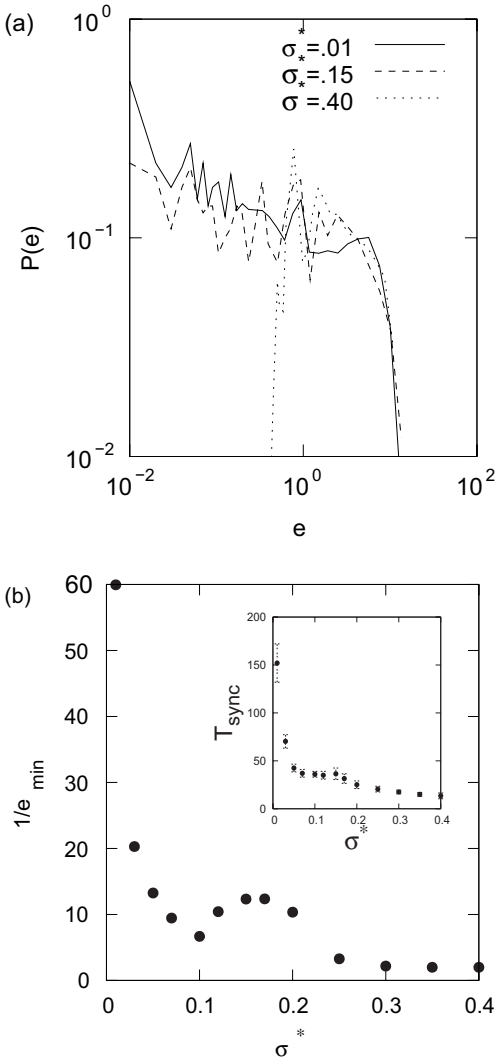

Fig. 6. (a) Spectrum of the Laplacian matrix of networks evolved for different values of σ^*. (b) Dependence of the inverse of the smallest non-zero eigenvalue of the Laplacian matrix of the evolved network on σ^* and dependence of the time T_{sync} till 99% of the stationary degree of synchronization $\overline{r}$ is reached on σ^* (inset). In both panels data are averaged over 100 optimized networks and for the inset of (b) also over 10 independent random initializations of the phases per network.

gaps $g_j = |1/e_{j+1} - 1/e_j|$, $j = 1, ..., N-1$ between close to zero eigenvalues with small index j decay strongly with σ^*. Since communities of many different sizes are evolved it is not surprising that the spectra do not reveal such clear gaps between groups of distinct eigenvalues as, e.g., discussed in [26].

Of interest in the context of synchronization are also the eigenratio $e_{\max}/e_{\min}$ and the inverse of the smallest eigenvalue $1/e_{\min}$. For systems of identical oscillators the eigenratio determines the stability of the fully synchronized state [6] and the inverse of the smallest non-trivial eigenvalue has recently been established to be associated with the time to synchronization [30].

Data for the dependence of $1/e_{\min}$ on the coupling σ^* are shown in Figure 6b. One observes an initially strong

decay of $1/e_{\min}$ with σ^* for partially synchronizable networks which is followed by a short recovery in the region of the core-periphery networks and a further decay in the direction of the core only networks that allow for full synchronization. We also measured the average time T_{sync} till 99% of the stationary value of global synchronization $\overline{r}$ is reached. The dependence on σ^* (cf. inset of Fig. 6b) corresponds well with that of $1/e_{\min}$ on σ^*, thus corroborating the findings of [30] for the synchronization of non-identical oscillators. We thus observe that relaxation times are longest for locally partially synchronizable networks and shortest for the networks where global synchronization becomes possible.

Last, since there is not much variation in the dependence of the maximum degree on σ^* the maximum eigenvalue $e_{\max}$ stays roughly constant and the dependence of the eigenratio on σ^* mirrors that of $1/e_{\min}$ on σ^*.

2.4 Sensitivity to the parameter λ

All results presented above were obtained for the particular choice of $\lambda = 1/2$. We also experimented with different values of $0 < \lambda < 1$ to check the sensitivity of results to it. Though the actual structure of the evolved networks is found to depend on λ, the general observation that networks evolved for different coupling strength σ^* change in a systematic way from low to large σ^* is found to be very robust. Clearly, the larger the contribution of the local synchronizability, the longer cliquish community structures are retained. On the other hand a larger contribution of the global synchronizability favours a transition towards the core-periphery and core only structures for lower σ^*.

For the extreme case $\lambda = 0$ the synchronization measure R only includes local synchronization. Optimal system configurations in this case are always characterized by only local synchronization. On the other hand, the case $\lambda = 1$ corresponds to the situation discussed in [25].

3 Clustering and the onset of synchronization

One of the contentions of the previous section is that a high degree of clustering facilitates the onset of synchronization, but works counter to reaching full synchronization. During the optimization procedure we applied so far, clustering in the network topologies but also in the arrangement of native frequencies on them was generated. As we will show below, already the clustering of the coupling network strongly influences the onset of synchronization.

Till now, the trade-off between the onset of synchronization and full synchronization has only been related to the heterogeneity of the degree distribution [23,24]. The main cause of an early onset of synchronization in heterogeneous networks are hub nodes, which synchronize first. In this way they build a germ cluster of synchrony that progressively encompasses more and more nodes as the network reaches higher levels of synchronization. However,

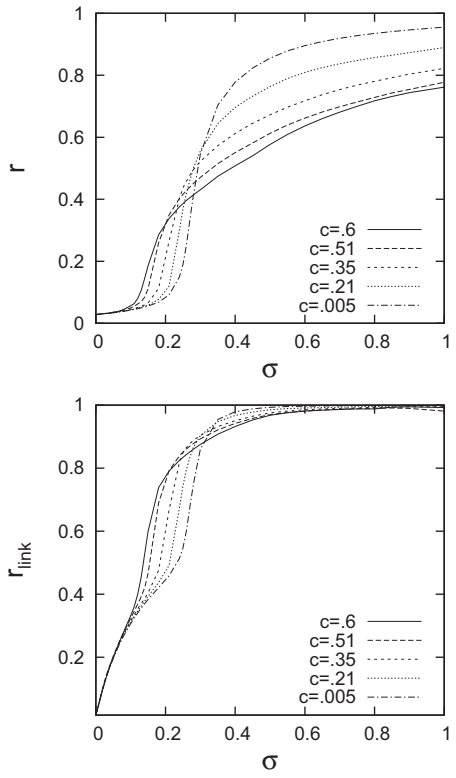

Fig. 7. Dependence of the of r and r_{link} on the coupling strength for networks with different degrees of clustering. Data are for networks of size $N = 1000$ with $\langle k \rangle = 5$. Each point represents an average over 10 random frequency combinations and 100 networks.

even though extremely large clustering seems to require the presence of hubs, networks can be highly clustered without having overly pronounced hub structures. Thus, relating clustering and the onset of synchronization and full synchronization points towards a mechanism different from the one previously described.

For a more detailed investigation of this problem networks of various degrees of clustering have to be constructed. In this we follow an approach in which we apply a network evolution procedure that gradually favors more and more cliquish configurations. The procedure consists of random link rewiring proposals (as in the optimization procedure in Sect. 2.1), that are accepted with probability p if they lead to an increase in the average clustering coefficient of the network and accepted with probability $1 - p$ otherwise. By varying the parameter p from $p = 0$ (bias towards small clustering), $p = 1/2$ (neutral) to $p = 1$ (strongest bias towards large clustering) ensembles of networks with different degrees of clustering can be generated. In the procedure we always make sure to only suggest rewirings if they lead to connected networks.

Figure 7 shows the dependence of r and r_{link} on σ for ensembles of networks with different levels of clustering. Clearly, for network topologies with larger clustering coefficient synchronization sets in for lower coupling strength while larger degrees of synchronization are harder

to achieve. Likewise, these networks exhibit a high degree of local synchronization for low coupling.

4 Conclusions

In this paper we have studied different trade-offs between local and global synchronization. Global synchronization is defined by the standard order parameter r, which measures the systemwide coherence of oscillators. Local synchronization, however, is defined in terms of the fraction of phase coherent linked pairs of oscillators as recently introduced in [23]. Depending on the structure of the coupling network the difference between both measures can be substantial as long as full synchronization has not been reached.

Defining the overall synchronizability R of networks as a combined measure of global and local synchronizability networks that optimize R for different coupling strengths σ^* have been evolved. The $r(\sigma)$ dependence of networks optimizing R for low and large coupling differs fundamentally. On networks evolved for low coupling a very early onset of synchronization is observed, but the transition to full synchronization is delayed to very large couplings. In contrast, networks evolved for large coupling have a later onset of synchronization, but rapidly reach the fully synchronized state after that. These findings support the conjecture that an early onset of synchronization and a rapid transition to the fully synchronized state are conflicting demands on network topology.

We found that networks that exhibit an early onset of synchronization typically have very expressed community structures, in which nodes of similar average native frequencies form cliques. These networks are typically relatively large and nodes associated with native frequencies of large magnitude tend to be at the periphery. In contrast, networks on which a rapid transition to full synchronization can be reached have no community structures, are not clustered, are marked by anticorrelations in the native frequencies of adjacent oscillators and are not cliquish [25]. In between both extremes networks with clique structures at the periphery and a unique central core realize intermediate trade-offs between an early onset and a rapid transition to a large degree of synchronization. These networks have large tree-like parts that distance few small remaining communities from the core.

The relation between clustering and the onset of synchronization is further supported by the experiments presented in the last section of the paper. There we first evolved networks with large clustering and then investigated the $r(\sigma)$-dependence for uncorrelated ensembles of oscillators. Large clustering of the network topology is demonstrated to be related to an early onset of synchronization, but also renders full synchronization more difficult. For networks with low clustering the onset of synchronization occurs later, but the transition is found to be steeper.

References

1. A.T. Winfree, *The Geometry of Biological Time* (Springer-Verlag, New York, 1980)
2. I. Blekhman, *Synchronization in Science and Technology* (ASME Press, New York, 1988)
3. S.C. Manrubia, A.S. Mikhailov, D.H. Zanette, *Emergence of Dynamical Order. Synchronization Phenomena in Complex Systems* (World Scientific, Singapore, 2004)
4. A. Pluchino, V. Latora, A. Rapisarda, Eur. Phys. J. B **50**, 169 (2006)
5. Y. Kuramoto, *Chemical Oscillations, Waves, and Turbulence* (Springer-Verlag, New York, 1984)
6. L.M. Pecora, T.L. Carroll, Phys. Rev. Lett. **80**, 2109 (1998)
7. Z. Liu, Y.-C. Lai, F.C. Hoppensteadt, Phys. Rev. E **63**, 055201 (2001)
8. M. Barahona, L.M. Pecora, Phys. Rev. Lett. **89**, 054101 (2002)
9. T. Nishikawa et al., Phys. Rev. Lett. **91**, 014101 (2003)
10. H. Hong et al., Phys. Rev. E **69**, 067105 (2004)
11. Y. Moreno, A.F. Pacheco, Europhys. Lett. **68**, 603 (2004)
12. D.-U. Hwang et al., Phys. Rev. Lett. **94**, 138701 (2005)
13. J.G. Restrepo, E. Ott, B.R. Hunt, Phys. Rev. E **71**, 036151 (2005)
14. A.E. Motter, C.S. Zhou, J. Kurths, Europhys. Lett. **69**, 334 (2005)
15. D.-S. Lee, Phys. Rev. E **72**, 026208 (2005)
16. M. Chavez et al., Phys. Rev. Lett. **94**, 218701 (2005)
17. L. Donetti, P.I. Hurtado, M.A. Muñoz, Phys. Rev. Lett. **95**, 188701 (2005)
18. C.S. Zhou, A.E. Motter, J. Kurths, Phys. Rev. Lett. **96**, 034101 (2006)
19. D. Newth, M. Brede, Complex Systems **16**, 317 (2006)
20. P.M. Gleiser, D.H. Zanette, Eur. Phys. J. B **53**, 233 (2006)
21. G. Korniss, Phys. Rev. E **75**, 051121 (2007)
22. C. Zhou, J. Kurths, Chaos **16**, 015104 (2006)
23. J. Gómez-Gardenes, Y. Moreno, A. Arenas, Phys. Rev. Lett. **98**, 034101 (2007)
24. J. Gómez-Gardenes, Y. Moreno, A. Arenas, Phys. Rev. E **75**, 066106 (2007)
25. M. Brede, (2007) to appear in Phys. Lett. A, DOI: `http://dx.doi.org/10.1016/j.physleta.2007.11.069`
26. A. Arenas, A. Diaz-Guilera, C.J. Pérez-Vicente, Phys. Rev. Lett. **96**, 114102 (2006)
27. S. Boccaletti, M. Ivanchenko, V. Latora, A. Pluchino, A. Rapisarda, Phys. Rev. E **75**, (2007) 045102(R)
28. P. Erdös, A. Rényi, Publ. Math. Inst. Hung. Acad. Sci. Ser. A **5**, 17 (1960)
29. D.J. Watts, S.H. Strogatz, Nature **393**, 440 (1998)
30. J.A. Almendral, A. Diaz-Guilera, New J. Phys. **9**, 187 (2007)